Office of Naval Research
Contract Nonr-1841(35)
Technical Report No. 6

DSR 7618

THE STRENGTH OF MARTENSITE

By
P. G. Winchell
Morris Cohen

1 March 1962
Department of Metallurgy
Massachusetts Institute of Technology
Cambridge, Massachusetts

THE STRENGTH OF MARTENSITE*

P. G. Winchell+ and Morris Cohen+

ABSTRACT

Iron-nickel-carbon alloys were selected to determine the role of carbon in the strengthening of virgin (untempered) martensite. The carbon content ranged from nil to almost 1 w/o C, while the nickel content was varied in the opposite sense to adjust the M_s temperature to -35° C. The martensites, thus formed at subzero temperatures, were maintained at low-temperature levels for the studies. Under these conditions, the axial ratio of the tetragonal lattice is found to increase with the carbon concentration, but there is also an extra tetragonality which is independent of carbon and which is thought to result from the presence of stacking faults. The extra tetragonality disappears on aging above room temperature where the regular tempering reactions occur.

The strength of unaged martensite increases rapidly as a function of carbon content, but levels off at about 0.4 w/o C. The carbon-strengthening is insensitive to the test temperature, and requires no prior diffusion or segregation of the carbon atoms. Thus, the carbon-dependent strengthening of virgin martensite can be described as a solid-solution hardening phenomenon. The fine structure of the martensite is thought to be a contributory factor in the overall strengthening. In addition, at temperatures above approximately -60° C, age hardening due to carbide precipitation provides a further component of strengthening which increases with the carbon content, but this increment is relatively small compared to the solid-solution effect.

---

* This paper is based on a thesis submitted by P. G. Winchell in September 1958 for the degree of Ph.D. in Metallurgy at the Massachusetts Institute of Technology. The research was conducted under sponsorship of the Office of Naval Research through Contract No. Nonr-1841-35.

+ Of the authors, P. G. Winchell is Assistant Professor in the School of Metallurgical Engineering at Purdue University, Lafayette, Indiana, formerly a graduate student in the Department of Metallurgy, Massachusetts Institute of Technology; Morris Cohen is Professor in the Department of Metallurgy, Massachusetts Institute of Technology, Cambridge, Massachusetts

INTRODUCTION

Virgin or untempered martensite produced by the diffusionless transformation of iron-carbon austenitic solid solutions is the basis of hardened steel. Yet, there is little actual knowledge about the strength properties of untempered martensite, both because of the brittleness of this phase and the difficulty of avoiding carbon diffusion in the martensite after its formation. In most plain carbon and alloy steels, the M_s is high enough for the martensite to undergo some diffusional changes even during rapid quenching. Further diffusion or carbide precipitation may occur on aging before the first measurements can be completed.

The hardness and strength of hardened steel are very dependent on the carbon content of the austenite from which the martensite is generated[1,2]. Both the extent and the mechanism of this hardening have been the subject of considerable thought[3,4], but it is still not clear whether virgin martensite (free from inadvertent aging or carbide precipitation) has the extraordinary strength that characterizes hardened steel. To answer this question unequivocally, it is necessary to inhibit, or allow for, any diffusional processes which might otherwise obscure the essential nature of the freshly formed martensite.

This problem was resolved in the present investigation by designing a series of iron-nickel-carbon martensites which could be produced, and studied, at subzero temperatures without being warmed back to room temperature. It was found that aging phenomena involving carbon diffusion can contribute materially to the strength of martensite at test temperatures above -60° C, but that the main strengthening factor is the solid-solution hardening of the carbon in the martensitic lattice. Even at temperatures well below -60° C, the as-formed martensites are characteristically strong, the degree of strengthening depending on the carbon content.

NATURE OF THE MARTENSITES INVESTIGATED

Alloy Preparation

The alloy compositions studied are listed in Table I, together with the austenitizing temperatures and other relevant information. Some of the alloys were vacuum-melted in 200 gram batches, using Ferrovac E iron, reagent grade nickel, and spectrographic carbon. These heats were chill cast, annealed at 900° C in evacuated vycor tubes for a total of about 50 hours, swaged to 0.090-inch diameter wire, and centerless ground to 0.070 inches. The wire samples were then austenitized (see Table I) in evacuated vycor or quartz capsules and water quenched in the capsules.

TABLE I - DESCRIPTION OF ALLOYS INVESTIGATED

w/o Carbon	w/o Nickel	Melting Practice V = Vacuum A = Air	Austenitizing Temp °C	Use
0.004	33.7	V	900 ± 2	Cast Single Crystals of Austenite for X-ray Diffraction
0.01	31.5	V	1400 ± 30	Strain-Anneal Single Crystals of Austenite for X-ray Diffraction
0.02	30.8	V	900 ± 2	Electrical Resistivity Measurements and Tensile Tests
0.02	30.5	A	900 ± 2	Compression and Hardness Tests
0.06	29.8	V	900 ± 2	Cast Single Crystals of Austenite for X-ray Diffraction
0.08	28.4	V	900 ± 2	Electrical Resistivity Measurements and Tensile Tests
0.14	27.1	V	900 ± 2	Cast Single Austenite Crystals for X-ray Diffraction
0.20	27.3	V	900 ± 2	Cast Single Austenite Crystals for X-ray Diffraction
0.22	27.4	V	900 ± 2	Electrical Resistivity Measurements and Tensile Tests
0.23	26.8	A	900 ± 2	Compression and Hardness Tests
0.28	24.5	V	900 ± 2	X-ray Powder Patterns and Electrical Resistivity Measurements

w/o Carbon	w/o Nickel	Melting Practice V = Vacuum A = Air	Austenitizing Temp °C	Use
0.30	25.3	V	900 ± 2	X-ray Powder Patterns
0.39	22.9	V	900 ± 2	X-ray Powder Patterns
0.40	23.0	V	900 ± 2	X-ray Powder Patterns
0.40	23.3	A	1000 ± 5	Compression and Hardness Tests
0.42.	23.0	V	1350 ± 30	Strain-Anneal Single Austenite Crystals for X-ray Diffraction
0.45	23	V	900 ± 2	Cast Single Austenite Crystals for X-ray Diffraction
0.48	20.3	V	900 ± 2	X-ray Powder Patterns and Electrical Resistivity Measurements
0.59	19.2	A	1100 ± 5	Compression and Hardness Tests
0.63	19.0	V	1000 ± 5	X-ray Powder Patterns and Electrical Resistivity Measurements
0.68	19.0	V	1350 ± 30	Strain-Anneal Single Austenite Crystals for X-ray Diffraction
0.82	16.7	A	1100 ± 5	Compression and Hardness Tests
0.96	15.1	V	1000 ± 5	X-ray Powder Patterns and Electrical Resistivity Measurements

These specimens were employed for lattice-parameter measurements, tensile tests, electrical-resistivity aging runs, and M_s determinations.

In addition, 30-pound heats were induction-melted in air, and hot worked to 5/8-inch diameter bars. This stock was used for hardness and compression tests. Small pieces of the bars were further reduced by swaging to 0.090 inches in diameter and centerless grinding to 0.070 inches, thus providing electrical-resistance specimens for checking the M_s temperatures.

Significant differences in behavior corresponding to the differences in melting practice were not observed. The following figures which present the experimental data also show the alloy compositions on which the data are based. The austenitic grain size was ASTM 5-6 for carbon contents below 0.4 w/o, ASTM 2-4 at 0.4 w/o C, and ASTM 1 for carbon contents above 0.4 w/o.

Iron-nickel-carbon alloys with an M_s of approximately -35° C were selected for most of the measurements because the corresponding transformation-temperature range is low enough to minimize self-tempering, and yet is high enough to permit 80 - 90% martensite to form on cooling in liquid nitrogen (-195° C). The compositions of this series varied from 0.01 to 0.96 w/o C and (in the opposite sense) from 31.5 to 15.1 w/o Ni.

The Lattice of Martensite

For preliminary studies, polycrystalline austenitic specimens were prepared from the water-quenched wires by etching them down to 0.025 inches in diameter. These samples were then cooled in liquid nitrogen to form martensite, and were x-rayed at room temperature in a Debye-Scherrer camera. All of the diffraction lines could be accounted for on the basis of body-centered tetragonal martensite and face-centered cubic austenite. The individual c and a parameters of the martensite were found to be influenced by the nickel content, but the c/a ratio (which could be measured more accurately than the separate c and a values) was only sensitive to the carbon content, as shown in Figure 1A.

The results of Figure 1A were verified and extended to much lower carbon levels by producing martensite from single crystals of austenite and using an oscillation x-ray technique[5-7]. Only one set of martensitic lattice orientations is generated from a single crystal of austenite because of the specific lattice relationships between the parent phase and the transformation product. In iron-base alloys, this set has clusters of $\langle 001 \rangle_M$ directions around each $\langle 100 \rangle_A$, and clusters of $\langle 100 \rangle_M$ directions around each $\langle 110 \rangle_A$. Suitable orientations and oscillations of the specimen can be selected so that the $\{002\}_M$ diffraction

line is recorded without the $\{200\}_M$ line, and vice versa. The c/a ratio was determined from these measurements. If the two lines were obtained simultaneously on the same film, the resulting doublet would be seriously overlapped and the small tetragonality existing at low carbon contents could not be ascertained.

The austenitic crystals required for this technique were grown either as large grains from slowly cooled melts or from chill-cast ingots by straining 1% and annealing for 24 hours at 1350° C. Rod-shaped specimens were cut from these crystals with axes along the $\langle 100 \rangle_A$ direction, and etched to 0.025 inches in diameter. The crystals were then oriented in a Unicam camera, quenched in place to -100° C to form martensite, and maintained at -100° C while an $\{002\}_M$ x-ray oscillation pattern was recorded. The $\{200\}_M$ x-ray oscillation pattern, which was not particularly affected by aging or tempering, was also recorded at -100° C, but after the martensitic sample had been returned to room temperature in order to remove the previously exposed film. The c/a ratios of the virgin iron-nickel-carbon martensites (M_s = -35° C) determined in this way are shown in Figure 1B.

The lines in Figures 1A and 1B conform to the equation:

$$c/a = 1.005 + 0.045 \text{ (w/o C)} \qquad (1)$$

It is to be noted that the martensite in these iron-nickel-carbon alloys is 0.005 more tetragonal than in plain-carbon and low-alloy steels, and that this extra tetragonality exists even at extremely low-carbon contents. This anomalous enhancement in axial ratio is not due to the high nickel contents of the alloys under study, but is a consequence of the low transformation temperatures involved.

The indications are that the extra tetragonality is apparent rather than real, and that it is a diffraction effect resulting from the presence of stacking faults on the $\{112\}_M$ plane[8]. If α is the probability of a stacking fault occurring on the $\{112\}_M$ plane, the corresponding shift in the relative positions of the $\{200\}_M$ and $\{002\}_M$ lines causes an anomalous change in the c/a ratio of $+0.21\ \alpha$. In a similar sense, faults on the $\{211\}_M$ plane would lead to an anomalous change in the c/a ratio of $-0.11\ \alpha$. Of these two possibilities, the former is the more likely because the observed increment in c/a is positive. If stacking faults on the $(112)_M$ plane are responsible for the extra tetragonality shown in Figure 1, then $\alpha^{-1} = 0.21/0.005 = 40$; i.e., a stacking fault occurs on about every 40th $(112)_M$ plane in these martensites.

Assuming, then, that the 0.005 increment in the axial ratio is not a manifestation of true tetragonality caused

by interstitial carbon atoms, equation 1 can not be rewritten:

$$c/a = 1.000 + 0.045 \text{ (w/o C)} \qquad (2)$$

which is exactly the same relationship reported by Roberts et al[6]. The new fact established here is that the tetragonality due to carbon atoms extends down to levels well below 0.1 w/o C. There is no indication of a body-centered cubic lattice in any of these virgin martensites, and the entire set of iron-nickel-carbon martensites may be regarded as a continuous series of body-centered tetragonal solid solutions.

By means of transmission electron microscopy, fine twins have been noted in martensites of the type under investigation here[9]. Unfortunately, these twins tend to obscure any direct substantiation of the postulated stacking faults. It can be said, however, that the twins or their interfaces do not account for the anomaly in the c/a ratio[8]. As will be pointed out later, the extra tetragonality starts to disappear as the martensite is heated slightly above room temperature, whereas the twinned structure remains[9].

Formation and Tempering (Aging) of the Martensites

The progress of both the martensitic and tempering reactions was traced by electrical-resistance measurements on 0.070-inch diameter wire specimens with a Kelvin

double bridge. These measurements were made during step-cooling to determine the M_s and to follow the course of the subsequent transformation. In all cases, the observed transformation started with a burst, and the M_s temperatures occurred in the range of -30 to -40° C. For the tempering reactions, the resistance changes were observed isothermally ($\pm$ 0.05° C) in the following way: The sample was austenitized in an evacuated capsule, quenched to room temperature and broken out of the capsule, connected to the bridge, and then quenched in liquid nitrogen for 5 minutes (during which its electrical resistivity was measured). After this treatment, the martensitic sample was up-quenched to the predetermined aging (tempering) temperature and the resistance was measured at that temperature for three hours. Then the specimen was requenched into liquid nitrogen where its resistance was determined again. Two examples of resistivity changes during such aging are shown in Figure 2. The differences between the resistivities at -195° C before and after the aging treatment are plotted in Figure 3.

At very low temperatures, -90° C and below, isothermal martensite formation[10,11] dominates the resistivity changes, and there is a resulting decrease in resistivity on aging. In Figure 2A for 0.02 w/o C, the resistivity decreases at all temperatures, but alloys containing

0.08 to 1 w/o C exhibit a positive component in resistivity on aging in the temperature range of -60° to about +40° C. Figure 2B for 0.48 w/o C illustrates these trends. A decrease in resistivity occurs at still higher temperatures and at longer times. Both the increase and subsequent decrease in resistivity due to aging are dependent on carbon content, as summarized in Figure 3.

The c/a ratios observed after aging at room temperature and at 100° C are given in Figures 4A and 4B as a function of carbon content. These results can be compared with those for virgin martensite in Figure 1B. Figure 4A shows that two axial ratios exist in martensite which has been aged at room temperature, at least for carbon contents between 0.2 and 0.45 w/o. This situation has been previously found in iron-carbon martensites after tempering at higher temperatures[5-7]. At low carbon levels, no experimental evidence for two separate axial ratios is to be expected because the corresponding diffraction lines cannot be resolved. At high carbon levels, the smaller axial ratio does not appear during room-temperature aging, but it does emerge after tempering at 60° C for 1 hour. Figure 4B indicates that the higher axial ratio disappears after tempering at 100° C for 1 hour. The axial ratio which remains is similar in magnitude to the smaller of the

previous two, but is actually somewhat larger for carbon contents above 0.2 w/o, and decreases as shown for carbon contents below 0.2 w/o. After this treatment, the extra tetragonality has vanished, and the axial ratios depict the end of the first stage of tempering in which the precipitation of epsilon carbide from martensites containing more than about 0.2 w/o C has reduced the dissolved carbon content to 0.2 w/o. At the same time, as the dissolved carbon content approaches zero, the axial ratio now approaches unity, instead of the previous 1.005, thus suggesting that the postulated stacking faults in the virgin martensite can anneal out at relatively low tempering temperatures. The removal of stacking faults could account for part of the observed decrease in resistivity at the higher aging temperatures (Figure 2), particularly in the low-carbon martensites, but inasmuch as the decrease becomes more pronounced with increasing carbon content, it must be due mainly to the carbide precipitation that attends the first stage of tempering.

Attention is now drawn to the increase in electrical resistivity observed when the higher carbon martensites are aged at intermediate temperatures, as in Figures 2B and 3. For purposes of discussion, three possible explanations may be considered: (a) a decrease in the degree of order existing in the martensitic solid solu-

tion[12]; (b) growth or spreading of stacking faults[13]; or (c) initial stages of carbide precipitation[14].

The carbon atoms in tetragonal martensite are located in only one of the three available sets of octahedral interstitial sites[15]. Such preferred or ordered sites are $00\frac{1}{2}$ and $\frac{1}{2}\frac{1}{2}0$ positions in the martensitic lattice. Disordering would then consist of carbon atoms moving from their initial set of sites into a more random arrangement among the three sets, and the tetragonal lattice would degenerate to cubic symmetry. According to Zener[16], the elastic interaction of the strain fields due to the carbon atoms in the preferred sites are responsible for maintaining the order. This interaction decreases with decreasing carbon content, and consequently at any given temperature any disordering would be expected to be most pronounced at low-carbon levels. However, even on tempering up to 100° C, the low-carbon martensites remain characteristically tetragonal in relation to the carbon content (Figure 4B). It is, therefore, quite unlikely that a cubic structure indicative of disorder could form in the subzero aging range where the increase in resistivity is found.

Stacking-fault growth may also increase the electrical resistivity. However, to be consistent with the tendency of the apparent c/a ratio to decrease on heating,

the stacking-fault growth would have to occur on $\{211\}_M$ planes, instead of on the $\{112\}_M$ planes where the faults must lie in order to account for the extra tetragonality in the first place. As discussed previously, the progressive disappearance of the extra tetragonality on heating is better explained by the removal of $\{112\}_M$ stacking faults, but this would be expected to cause a decrease rather than an increase in resistivity.

The simplest and most satisfactory explanation of the increase in resistivity under consideration is that it is caused by the initial stages of the carbide-precipitation process. In other words, the aging which can be detected in virgin martensite at subzero temperatures is merely the very early part of carbide precipitation in the first stage of tempering which has been studied in detail at room temperature and above[5-7]. Actually, many precipitation systems are known in which the resistivity first increases and then decreases during the reaction[14].

MECHANICAL PROPERTIES

Experimental Procedures

The flow stress at 0.006 plastic strain was measured under tensile and compressive loading. Tensile tests were confined to carbon contents below 0.2 w/o C because

brittle failure preceded appreciable plastic flow at higher carbon levels. These tests were performed in refrigerated liquid baths on wire specimens of the vacuum-melted stock. The gage section was 0.0425 ± 0.0005 inches in diameter by 1-1/4 inches long. Strain was measured by crosshead motion.

Compression tests over the entire carbon range were carried out between polished tungsten carbide platens in a subpress which was cooled in a refrigerated liquid bath and loaded by a universal testing machine. The test specimens were of air-melted stock in the form of cylinders 0.400 inches in diameter by 0.900 inches long. Strain was measured by the calibrated change in inductance of a solenoid whose core displacement was activated by the change in diameter of the specimen.

In both test procedures, the elastic deformation of the testing equipment contributed to the measured strain. The stress at 0.006 plastic strain was selected as a criterion of the yield strength because it was less sensitive to this extra deformation than was the conventional stress at 0.002 plastic strain.

The heat treatment, cold treatment and subsequent manipulation of these specimens were designed to assure solution of all carbon in the austenite, to produce regulated quantities of martensite, to subject the martensite-austenite mixtures to controlled aging cycles

at subatmospheric temperatures, and to carry out the mechanical testing of these specimens without prior warming back to room temperature. After testing, the volume percent martensite was determined within $\pm$ 5% by x-ray intensity measurements or by quantitative metallography on longitudinal samples taken from lightly strained parts of the test pieces.

Effect of Nickel

Because appreciable nickel variations are necessary to maintain the M_s temperature at -35° C when the carbon is changed from 0.01 to 0.96 w/o, the influence of nickel itself on the mechanical properties of martensite should be known. This effect was determined in binary iron-nickel alloys to provide some indication of the solution hardening contributed by the nickel to the iron-nickel-carbon martensites. Compression tests showed that the flow stress at 0.006 plastic strain changes by no more than about 10,000 psi between 10 and 30 w/o nickel, the entire range of interest here. This variation may be neglected in the following considerations because it is swamped out by the effect of carbon.

Effect of Carbon

In the first instance, the flow stress of martensite-austenite aggregates was measured at 0° C for about ten different martensite contents in each of several alloys

after aging for 3 hours at 0° C. The range of martensite contents was achieved by subcooling the initially austenitic specimens to different temperatures below M_s prior to the aging and testing at 0° C. For each alloy, the flow stress thus determined was found to be a linear function of the percent martensite, and the flow stress of 100% martensite was obtained by the extrapolation of least-square straight lines, as shown in Figure 5*.

The extrapolated results are plotted as a function of carbon content in curve (1) of Figure 6. The standard deviations are also indicated. It will be noted that the tensile and compressive tests are mutually consistent over the low-carbon range where both types of tests can be compared. Hence, in the higher-carbon range where the specimens were too brittle for tensile testing under the difficult conditions at hand, it is reasonably safe to rely on the compressive data for the flow stresses. It is evident from Figure 6 that the yield strength of martensite, at least after aging at 0° C, increases rapidly with carbon content, but at a decreasing rate.

---

* The flow stresses, as measured, were affected somewhat by the stress-induced transformation of retained austenite in the tensile tests, but not to the extent of causing serrations in the stress-strain curves. Moreover, any possible error due to this source was eliminated by the extrapolation to 100% martensite.

In the next series of tests, the contribution of the aging at 0° C involved in curve (1) of Figure 6 was investigated. At the same time, the test temperature was introduced as a variable. Austenitized tensile and compressive specimens were cooled to -195° C in order to generate the maximum amount of martensite (80 - 90%). One set of specimens was then tested at a series of temperatures from -195° C to 0° C, holding a minimal time (15 minutes) at each temperature (Q-curves in Figure 7). Another set of specimens was aged for 3 hours at 0° C and tested (A-curves in Figure 7) at the same temperatures employed for the first set.

Figure 7 shows that below about -60° C the temperature dependence of the flow stress is insensitive to the carbon content, and remains the same whether the martensite has been aged at 0° C or not. Above -60° C, the Q-curves indicate that strengthening occurs during the test; this is due to the entree of the aforementioned aging process. Also, as might be expected now, the magnitude of the effect depends on the carbon content, being absent in the two lowest-carbon alloys. When aging is intentionally applied, as at 0° C, the corresponding strengthening component is observed at all the test temperatures (compare the A-curves with the Q-curves in Figure 7). However, there is no such age-hardening effect in the two

lowest carbon alloys, presumably because of insufficient carbon.

It is quite evident, then, that the carbon-dependent strengthening of martensite, as denoted by curve (1) in Figure 6 contains a component of strengthening due to age hardening even when the aging and testing are conducted at 0° C. This component is nil if the carbon content is sufficiently low, but becomes appreciable as the carbon is raised. This phenomenon is further demonstrated in Figure 8 where hardness values, measured at -195° C, are plotted as a function of the aging temperature. Not only does the -195° C hardness of the virgin martensite increase with the carbon content as might be anticipated, but the age hardening above -60° C is quite pronounced except for the very lowest-carbon alloy. The extent of the age hardening reaches a maximum somewhat above room temperature, signifying that the subzero aging of virgin martensite is continuous with the well-known hardening observed during the first stage of tempering[6].

These hardness experiments confirm the suggested interpretation of the differences between the Q- and A-curves in Figure 7. If these differences are now divided by the fraction (0.8 - 0.9).of martensite present in the respective alloys, the strengthening contribution due to the aging at 0° C of 100% martensite may be estimated. These values can

then be subtracted from the corresponding points on curve (1) in Figure 6 to yield curve (2) which represents the strength of unaged or virgin martensite. The effect of carbon is still very striking; the strength is comparatively low when the carbon is nil but increases very rapidly with carbon content up to about 0.4 w/o C. As indicated in Figure 7, the strength of virgin martensite also increases with decreasing test temperature, but in view of the approximate parallelism of the several curves below -60° C, it may be concluded that the carbon-dependent strengthening is insensitive to the test temperature.

DISCUSSION OF RESULTS

The hardening mechanisms applicable to the strengthening of martensite by carbon may be divided into those which require the prior movement of carbon atoms and those which do not, the latter involving some form of solution hardening. The first group of mechanisms includes segregation of carbon atoms to individual dislocations, dislocation arrays, twin boundaries, stacking faults, or to other carbon atoms as in clustering and precipitation. The corresponding strengthening mechanisms (i.e., Cottrell locking, chemical interaction, and precipitation hardening) cannot be active in freshly formed martensite unless carbon

diffusion occurs before or during the test, and the extent of such diffusion should be greater, the higher the testing temperature. This effect is actually observed above about -60° C (Figures 7 and 8), but it is of secondary interest. At lower temperatures, the strengthening contribution of the carbon becomes independent of the test temperature, indicating that for martensites formed and tested below -60° C, the strengthening is not due to a temperature-dependent aging or carbon-segregation process.

Accordingly, consideration will now be given to possible mechanisms of solid-solution hardening which might be relevant here. One suggested mechanism for the strengthening of martensite by dissolved carbon is based on the strain-induced ordering (or disordering) of carbon atoms due to the stress fields of moving dislocations[17]. The energy of interaction between the stress field of the dislocation and the distortion produced by the repositioning of the carbon atoms has to be provided by the external stress, and could conceivably result in effective resistance to the passage of dislocations. However, the characteristic carbon-damping peak is absent in martensite[18], thus indicating that carbon atoms do not reorder, at least under the small strain variations used in an internal-friction test. Inasmuch as the damping effects are known to be insensitive to the applied strain, it appears that any reordering of carbon atoms by moving dislocations will

probably be confined to the dislocation cores where inelastic distortions occur. Unfortunately, the interaction of dissolved solute atoms with the core of a dislocation has not been elucidated. Flinn[19] has suggested that carbon atoms in martensite may be repositioned within the dislocation core as a result of the large displacements there. The repositioned carbon atoms may then be left in disordered positions as the dislocation moves away, and the required mechanical stress must be correspondingly increased to provide the additional energy. Since the number of carbon atoms that become disordered in this process and the increase in internal energy per disordered carbon atom are each expected to be proportional* to the carbon concentration, the strengthening should increase with the square of the carbon content, and the effectiveness of carbon should be smallest at low carbon levels. In contrast, that is where the rate of strengthening by carbon is a maximum.

Let us now consider the possible strengthening of martensite by interactions among the dissolved carbon atoms. Carbon pairs in which the atoms are separated by c, the long dimension of the tetragonal unit cell, possess a relatively high energy due to the unfavorable interaction

---

* Direct proportionality is to be expected if the strain in the martensite produced by the ordering of all the carbon atoms is essentially homogeneous.

of their lattice distortions[20]. This situation also prevails in the austenite, and hence unfavorable carbon pairs in the virgin martensite (inherited from the austenite) will be rare. In fact, if they should exist momentarily, little thermal energy would be necessary for their removal. On the other hand, as a result of a single slip of one Burgers vector, such pairs could be formed in the following numbers in a solid solution containing n carbon atoms per metal atom, with the carbon atoms being initially more or less randomly arranged among the permitted interstitial sites of the tetragonal lattice:

$$\text{Number of unfavorable carbon pairs per unit area of slip plane} = \frac{2dn^2}{a^2c} \qquad (3)$$

where d is the slip plane spacing and a^2c is the volume of the tetragonal unit cell (See Appendix for derivation of equation 3). If U is the energy associated with each unfavorable pair, then the extra energy necessary to move a dislocation over a unit area of slip plane requires an additional force, ΔF, per unit length of dislocation:

$$\Delta F = \frac{2dn^2}{a^2c} U \qquad (4)$$

Thus, the expected increase in the shear stress necessary to move the dislocation is:

$$\Delta\tau = \frac{2dn^2U}{ba^2c} \qquad (5)$$

where b is the Burgers vector.

An approximate upper bound may be placed on this effect by taking U as the activation energy for carbon diffusion. Under this assumption

$$\Delta\tau < 100 \text{ (w/o C)}^2 \text{ psi} \qquad (6)$$

Consequently, this mechanism predicts a hardening which is negligible at the carbon levels of interest. Furthermore, equation (6) indicates that the rate of strengthening by carbon should increase with the carbon content, whereas the experimental findings (Figure 6) show just the opposite.

It is also improbable that the carbon-strengthening of martensite is caused by an increase in lattice binding, sometimes referred to as an "intermetallic compound effect." Young's modulus of these martensites decreases with increasing nickel content, and also decreases with increasing carbon content. These changes suggest a decrease in lattice binding, if anything. Furthermore, in the compositions studied, it turns out that the influence of carbon on Young's modulus is relatively small compared to that of nickel, whereas the strengthening effects of these two elements in solution are quite the reverse.

Some significance may be attached to the fine layer-like twinned structure within the martensitic plates[9]. This structure appears to be absent in low-carbon iron-carbon

martensites, but it is present in low-carbon iron-nickel martensites[21]. Since the latter are relatively soft, hardening cannot be attributed primarily to the presence of such twins. The carbon in solution seems to be the main factor in the strengthening.

In view of the inadequacies of the hardening mechanisms discussed thus far, the authors have come to the conclusion that the strengthening of martensite by dissolved carbon atoms is a consequence of the limited but important flexibility of a dislocation line on the scale of atomic dispersion of the solute atoms[22]. It is thought that the dislocation bends slightly in response to the stress fields of the carbon atoms and requires additional force to move it up the resulting energy gradient.

In a study of the carbon-strengthening of ferrite (at constant grain size), Cracknell and Petch[23] made a calculation of the theoretical strengthening due to the elastic stress field of a dislocation interacting with the distortions caused by random carbon atoms; this gave 1×10^5 psi per w/o C, whereas 6×10^5 psi per w/o C was found experimentally. The latter figure is independent of the test temperature[24] and is to be compared with 2.3×10^6 psi per w/o C determined here for the unaged low-carbon martensite, which figure is also independent of the test temperature.

Elsewhere[25] the present authors have calculated the strengthening of martensite by dissolved carbon, using the same principle of solid-solution hardening[22], but obtaining the interaction between the elastic stress field of the carbon atoms and the distortion caused by the dislocation. In addition, the finely twinned structure of the martensitic plates was assumed to limit the dislocation length free to move under applied stress. A strengthening of 1.7×10^5 (w/o C)$^{1/3}$ was obtained which is in fair agreement with Curve 2 of Figure 6.

The rate of strengthening of martensite by dissolved carbon becomes small above 0.4 w/o C. This probably results from the circumstance that when the carbon atoms lie too close together, carbon-carbon interactions tend to diminish the stress field around any given carbon atom. Also more carbon atoms then reside within the

dislocation core, making the dislocation-solute atom interaction difficult to assess. These factors have not been taken into account in the theoretical treatments[22-24], and could well cause the rate of strengthening due to carbon to fall off rapidly at the higher-carbon concentrations.

It has been pointed out that diffusion-dependent aging or precipitation begins at temperatures as low as -60° C, and appreciable age hardening occurs above this temperature in carbon-bearing martensites. Precipitation hardening has long been recognized in high-carbon steels. Figures 6, 7 and 8 show that aging makes a contribution to the room-temperature strength at all but the lowest carbon levels; this component of strengthening undoubtedly comes into play in commercially hardened steels.

CONCLUSIONS

1. Iron-nickel-carbon martensites, as formed and studied below room temperature, are body-centered tetragonal down to extremely low carbon levels. There is also an extra tetragonality, independent of the carbon content, which appears to be due to the presence of stacking faults in the martensite.

2. Virgin martensite begins to undergo temperature-dependent aging above about -60° C, and if the carbon content is not too low, an increase in electrical resistivity occurs, followed by a decrease. These phenomena constitute the start of the well-known first

stage of tempering. On further aging above room temperature, the extra tetragonality vanishes and there is a discontinuous decrease in tetragonality, characteristic of the first stage of tempering.

3. Virgin martensite is strengthened by the solid-solution hardening of carbon atoms in the martensitic lattice. This carbon-dependent strengthening is insensitive to the test temperature, no prior diffusion or segregation of the carbon atoms being necessary. The rate of carbon-strengthening is a maximum at low-carbon levels, and is greater than the rate of carbon-strengthening in ferrite. The fine structure of the martensite appears to be a contributory factor in the overall strengthening.

4. The age-hardening of iron-nickel-carbon martensites above -60° C provides a component of strengthening which increases with the carbon content, but the increment is relatively small compared to the solid-solution strengthening.

ACKNOWLEDGMENTS

It is a pleasure to acknowledge the assistance of Messrs. G. Langford, S. Lorris, and M. Smith in carrying out the experimental work. The authors are also appreciative of the financial support of the Office of

Naval Research.

Further thanks are due to the Universal-Cyclops Steel Corporation for a Fellowship held by one of the authors, and to the Vanadium-Alloys Steel Company for the preparation of the air-melted heats of steel.

REFERENCES

1. J. L. Burns, T. L. Moore and R. S. Archer, "Quantitative Hardenability," Trans. ASM 26 (1938) 1.

2. A. E. Nehrenberg, Peter Payson and Peter Lilly, "Effect of Carbon and Nitrogen on the Attainable Hardness of Martensitic Steel," Trans. ASM 47 (1955) 785.

3. Albert Sauveur, The Metallography and Heat Treatment of Iron and Steel, Fourth Edition, Univ. Press, Cambridge (1935) 263.

4. N. H. Polakowski, "Observations on the Mechanical Behavior of Heat Treated Steel at High Hardness Levels," J. Iron and Steel Inst. 185 (1957) 67.

5. G. Kurdjumov and L. Lyssak, "Use of Monocrystals for the Study of Tempered Martensite," J. Tech. Phys. USSR 16 (1946) 1307.

6. C. S. Roberts, B. L. Averbach and Morris Cohen, "The Mechanism and Kinetics of the First Stage of Tempering," Trans. ASM 45 (1953) 576.

7. F. E. Werner, B. L. Averbach and Morris Cohen, "The Tempering of Iron-Carbon Martensite Crystals," Trans. ASM 49 (1957) 823.

8. O. J. Guentert and B. E. Warren, "X-Ray Study of Faults in Body-Centered Cubic Metals," J. Applied Physics 29, No. 1 (1958) 40.

9. P. M. Kelly and J. Nutting, "The Martensite Transformation in Steels," Proc. Roy. Soc. A 259 (1960) 45; also "The Morphology of Martensite," J.I.S.I. 197 (1961) 199.

10. E. S. Machlin and Morris Cohen, "Isothermal Mode of the Martensitic Transformation," Trans. AIME 194 (1952) 489.

11. Koshiro Sakamoto and Takesi Sugeno, "On the Lattice Imperfections Produced by Alloys," Osaka Univ. Mem. of the Inst. of Sc. and Ind. Res. XVI, (1959) 119.

12. T. Broom, "Lattice Defects and the Electrical Resistivity of Metals," Advances in Physics 3 (1954) 26.

13. A. H. Cottrell, "Interactions of Dislocations and Solute Atoms," Relation of Properties to Microstructure, ASM, Cleveland (1954) 131.

14. A. H. Geisler, "Precipitation from Solid Solutions of Metals," Phase Transformations in Solids, Smoluchowski, Mayer, Weyl, Editors, J. Wiley, New York (1951) 387.

15. Morris Cohen, "The Martensite Transformation," Phase Transformations in Solids, Edited by Smoluchowski, Mayer and Weyl, John Wiley and Sons, Inc., New York (1951) 588.

16. Clarence Zener, "Kinetics of the Decomposition of Austenite," Trans. AIME 167 (1946) 550.

17. G. Schoeck and A. Seeger, "The Flow Stress of Iron and its Dependence on Impurities," Acta Met. 7 (1959) 469.

18. Philip Stark, B. L. Averbach and Morris Cohen, "Influence of Microstructure on the Carbon Damping Peak in Iron-Carbon Alloys," Acta Met. 6 (1958) 149.

19. P. A. Flinn, Private Communication.

20. J. C. Fisher, "Elastic Interaction of Interstitial Atoms in Body-Centered Cubic Crystals," Acta Met. 6 (1958) 13.

21. M. H. Richman, Private Communication.

22. N. F. Mott and F. R. Nabarro, "Dislocation Theory and Transient Creep," Conference on the Strength of Solids, University of Bristol Report, N. F. Mott, Editor, Physical Society, London (1948) 1.

23. A. Cracknell and N. J. Petch, "Frictional Forces on Dislocation Arrays at the Lower Yield Point in Iron," Acta Met. 3 (1955) 186.

24. J. Heslop and N. J. Petch, "The Stress to Move a Free Dislocation in Alpha Iron," Phil. Mag. Ser. 8 (1957) 866.

25. P. G. Winchell and Morris Cohen, "Solid-Solution Strengthening of Martensite by Carbon," Electron Microscopy and Strength of Crystals, G. Thomas and J. Washburn, Eds., to be published by Interscience Publishers, Inc., N.Y.

APPENDIX

Derivation of Number of Unfavorable Carbon Atom Pairs Formed by Slip in Tetragonal Martensite

For reasons stated in the text, it is assumed that very few unfavorable pairs of carbon atoms will exist in freshly quenched tetragonal martensite, i.e., carbon atoms will avoid being simultaneously on the $+c/2$ and $-c/2$ sides of any given iron atom because this is a high-energy configuration. If slip is subsequently imposed on the martensite, there is a randomizing effect on the occupancy of the available interstitial sites, and unfavorable pairs of carbon atoms may be forced to form, at least momentarily. We should like to know how many of these pairs can be expected on a unit area of slip plane when slip of one Burgers vector occurs.

Let n = number of carbon atoms per metal atom

d = distance between slip planes

a^2c = volume of tetragonal unit cell

Since there is one available interstitial site per metal atom in body-centered tetragonal martensite, the probability that a given metal atom has a carbon atom in the $+c/2$ position is n. On the assumption that slip of one Burgers vector is sufficient to make the occupancy of a $-c/2$ site independent of whether the corresponding $+c/2$ site across the slip plane is also occupied,

the probability that the given metal atom will then have a carbon atom in the -c/2 position is also n. Hence, n^2 is the probability that both positions will be occupied concurrently after the unit slip.

Inasmuch as there are two metal atoms per unit cell, the effective volume per metal atom is $\frac{a^2c}{2}$, and the effective area per metal atom on the slip plane is $\frac{a^2c}{2d}$. There will then be $\frac{2d}{a^2c}$ metal atoms per unit area of slip plane. Thus:

Number of unfavorable carbon pairs per unit area of slip plane $= \frac{2dn^2}{a^2c}$

which is equation 3 in the text.

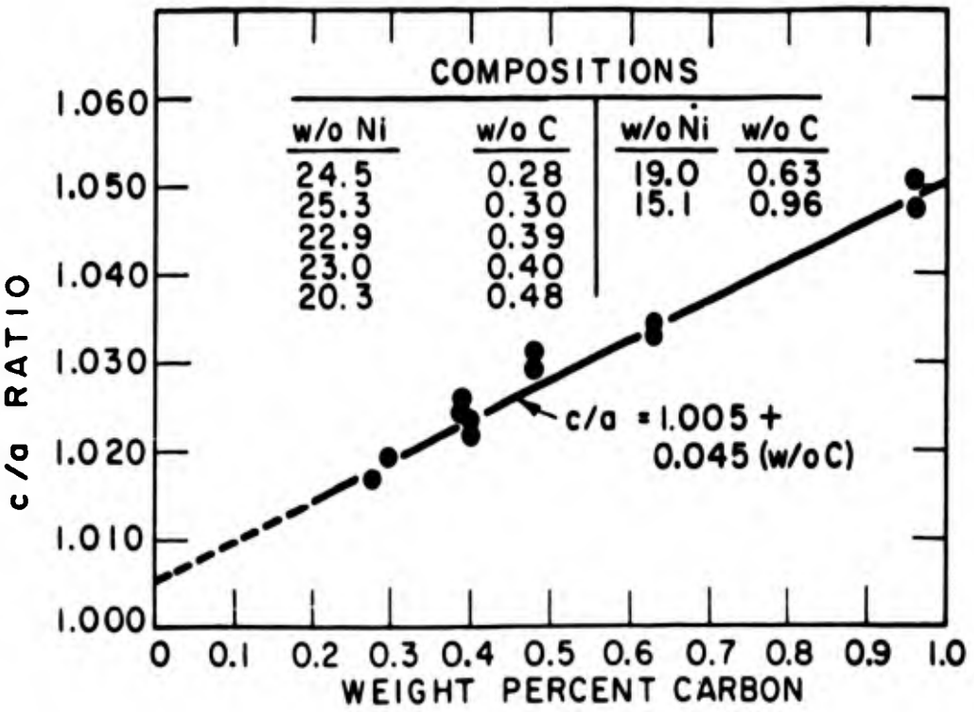

Fig. 1A c/a Ratios of Iron-Nickel-Carbon Martensite as Determined from Polycrystalline Specimens Transformed below −35°C and X-Rayed at Room Temperature

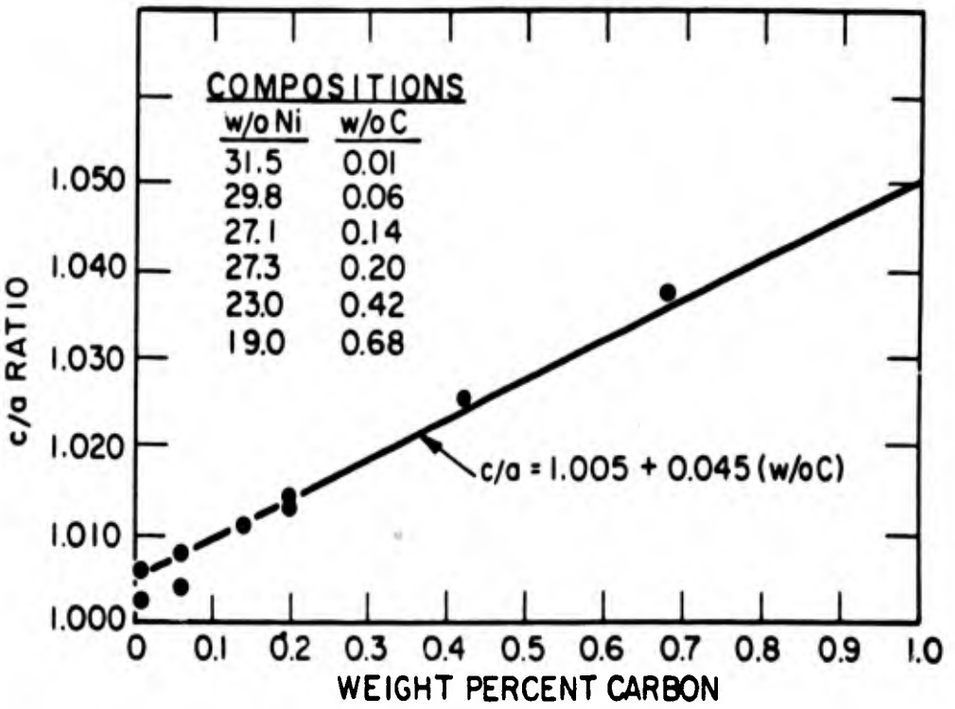

Fig. 1B c/a Ratios of Iron-Nickel-Carbon Martensites as Determined from Austenite Single Crystals Transformed Below −35°C and X-Rayed at −100°C

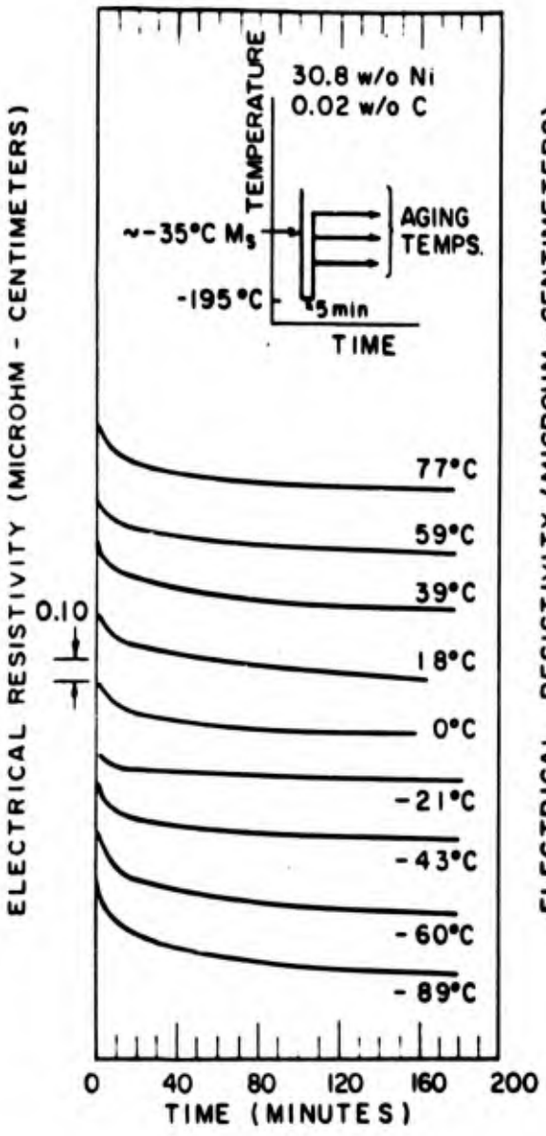

Fig. 2A

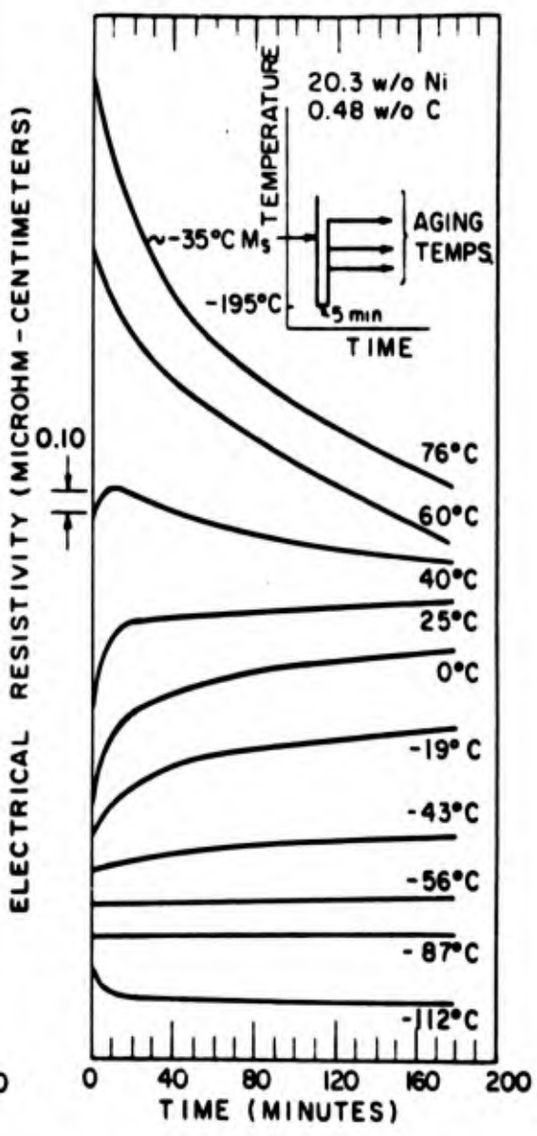

Fig. 2B

Change in Electrical Resistivity During Aging of Two Iron-Nickel-Carbon Alloys at the Temperatures Indicated after Precooling to −195°C. Vertical Positions of Curves are Arbitrary.

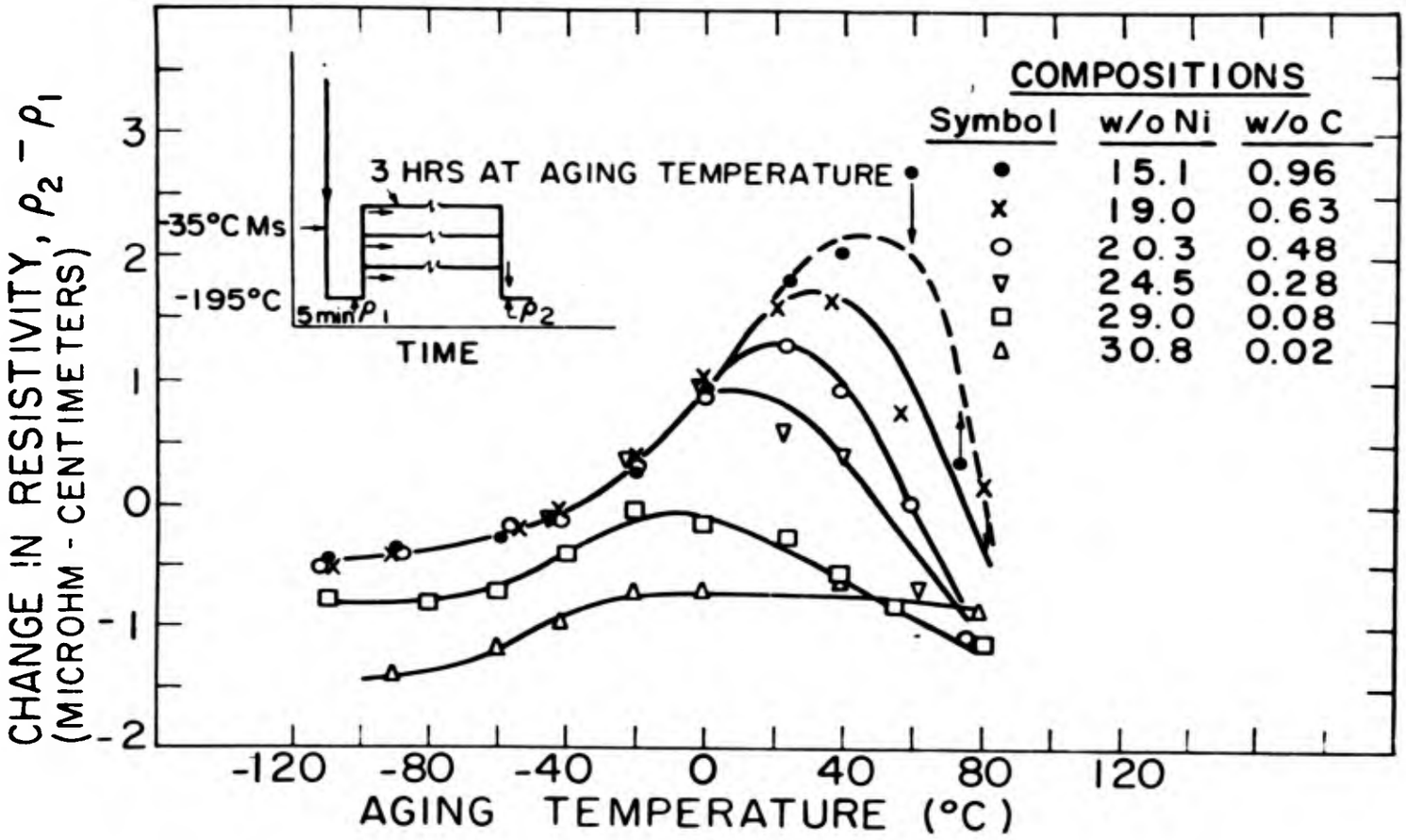

Fig. 3 Change in Electrical Resistivity as Measured at -195°C of Iron-Nickel-Carbon Alloys as a Function of Aging Temperature. Aging Time = 3 Hours

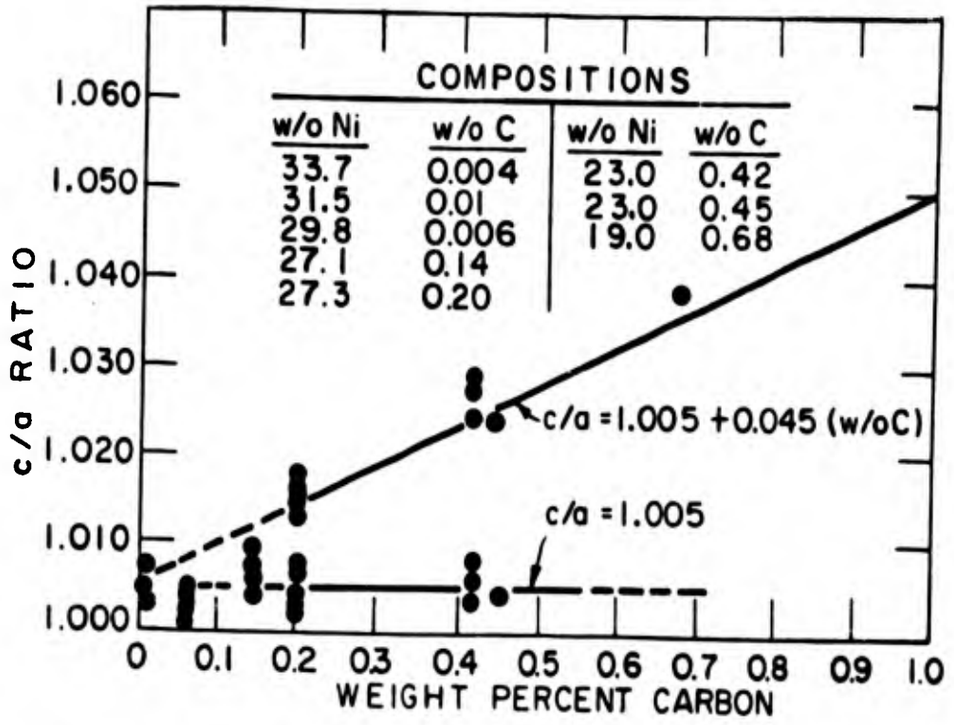

Fig. 4A c/a Ratios of Iron - Nickel - Carbon Martensites as Determined from Austenite Single Crystals Transformed Below - 35°C and Aged for 1 Hour at Room Temperature.

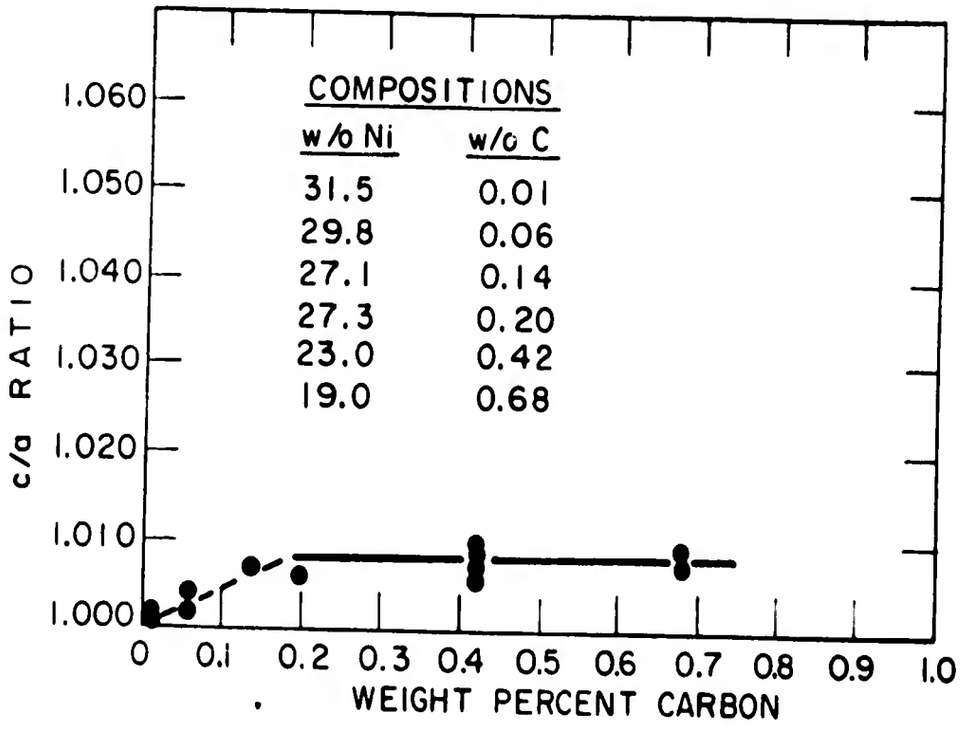

Fig. 4B c/a Ratios of Iron - Nickel - Carbon Martensites as Determined from Austenite Single Crystals Transformed Below - 35°C and Aged for 1 Hour at 100° C

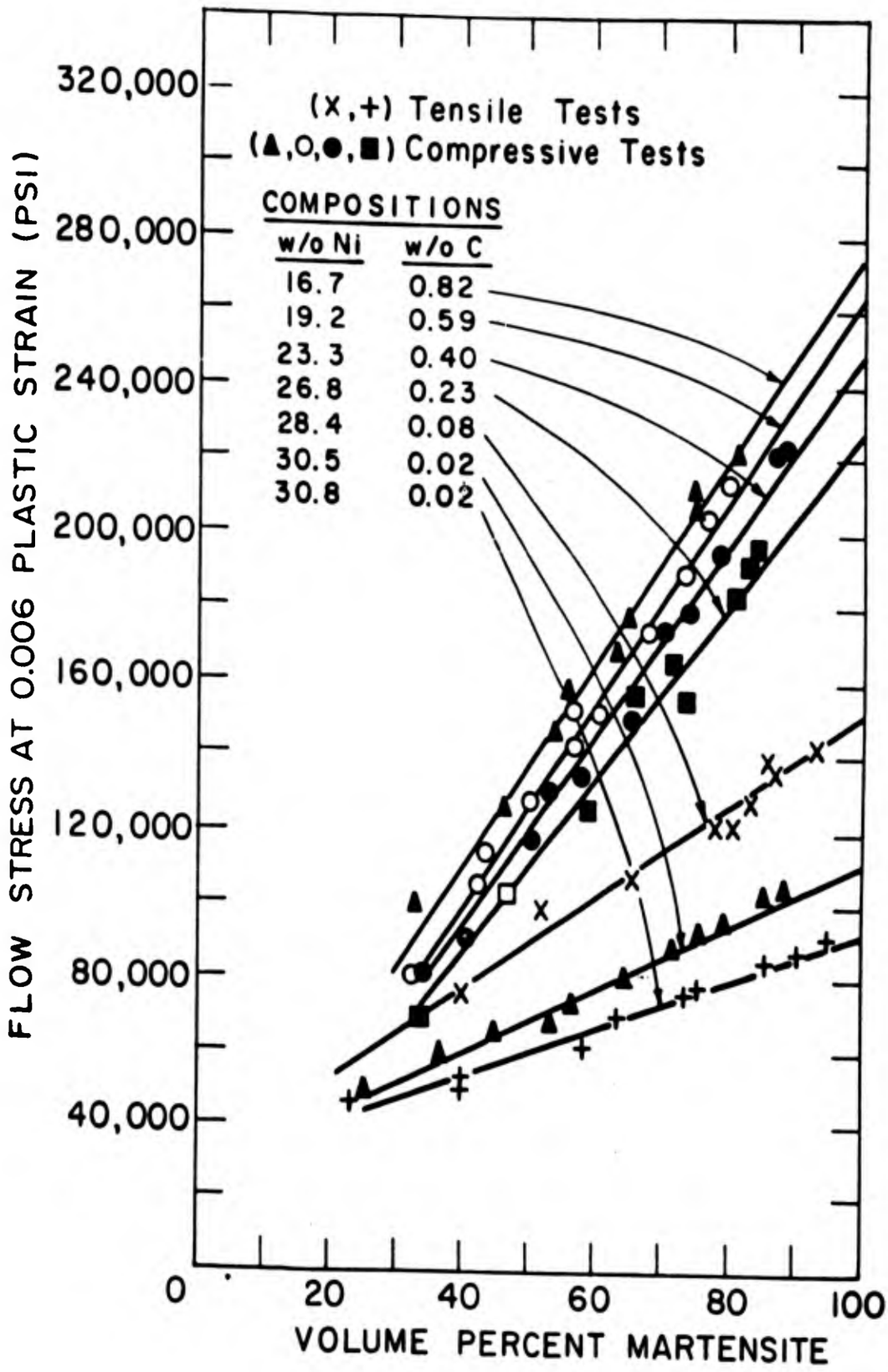

Fig. 5 Flow Stress (at 0.006 Plastic Strain) of Martensite - Austenite Mixtures after Aging 3 Hours at 0°C. Tested at 0°C.

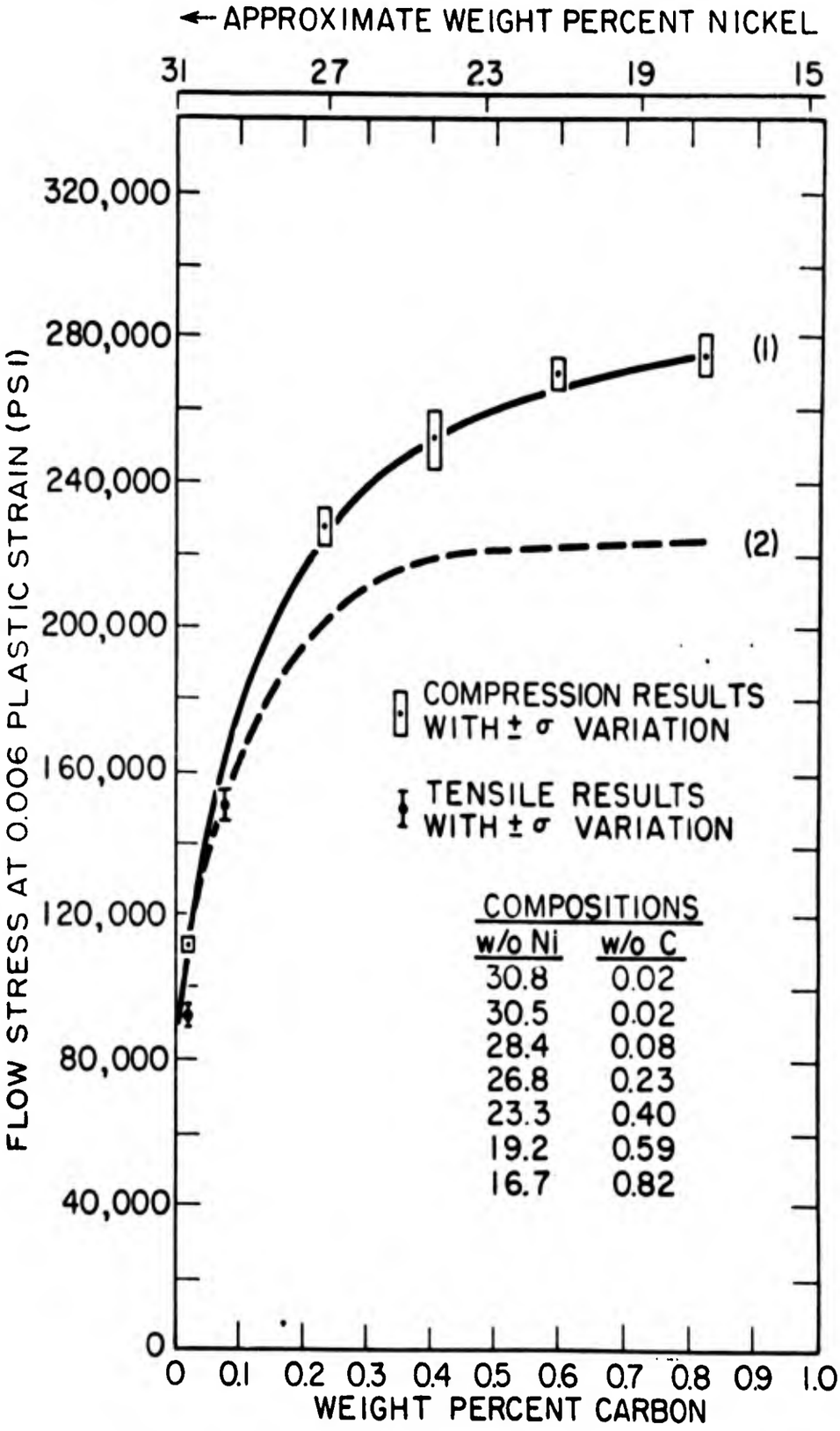

Fig. 6 Flow Stress (0.006 Plastic Strain) for 100 Percent Martensite at 0°C. Curve (1) - Experimental, Aged 3 Hours at 0°C. Curve (2) - Corrected for Aging.

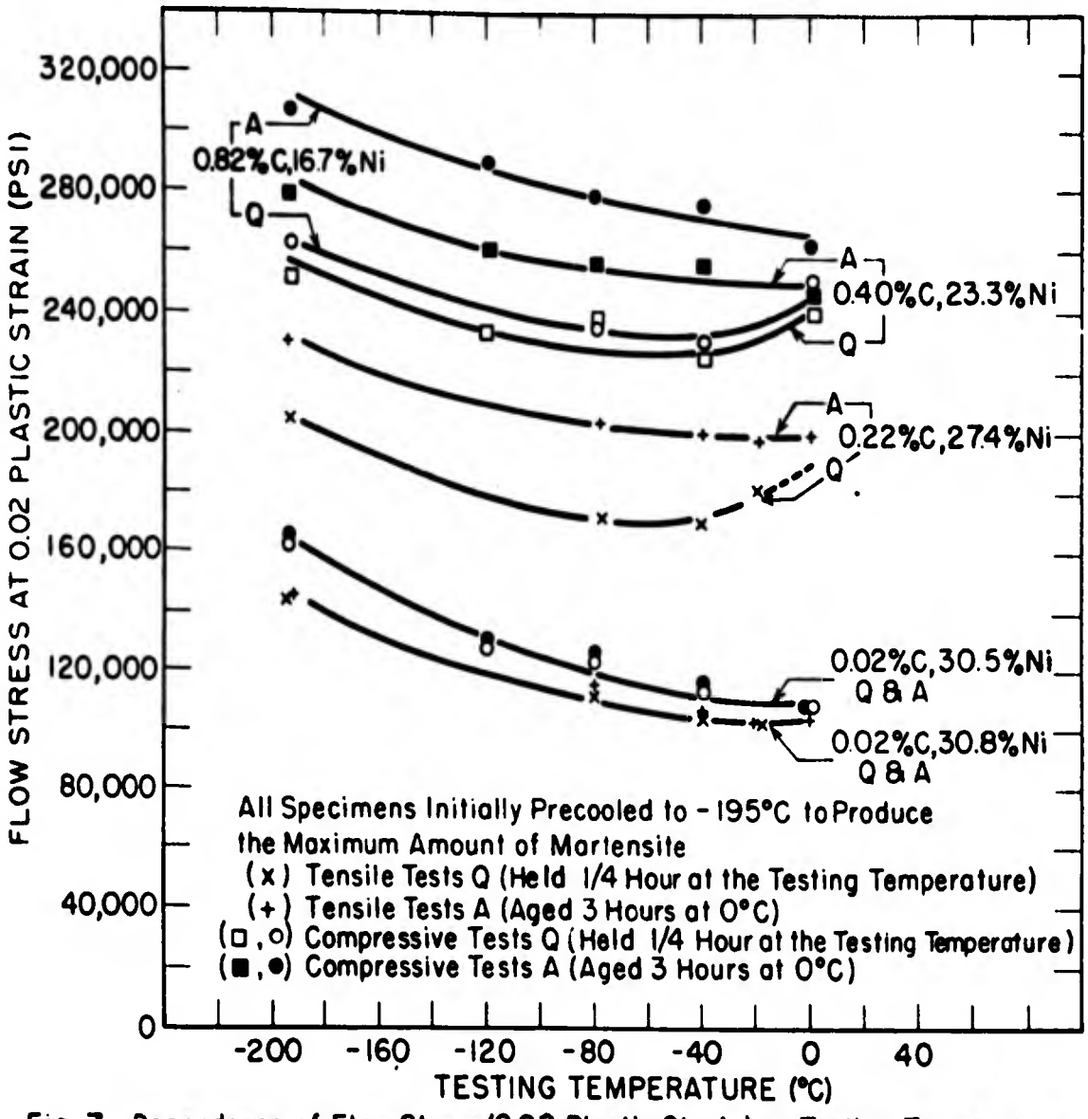

Fig. 7 Dependence of Flow Stress (0.02 Plastic Strain) on Testing Temperature for As-Quenched Alloys (Q) and for Aged Alloys (A).

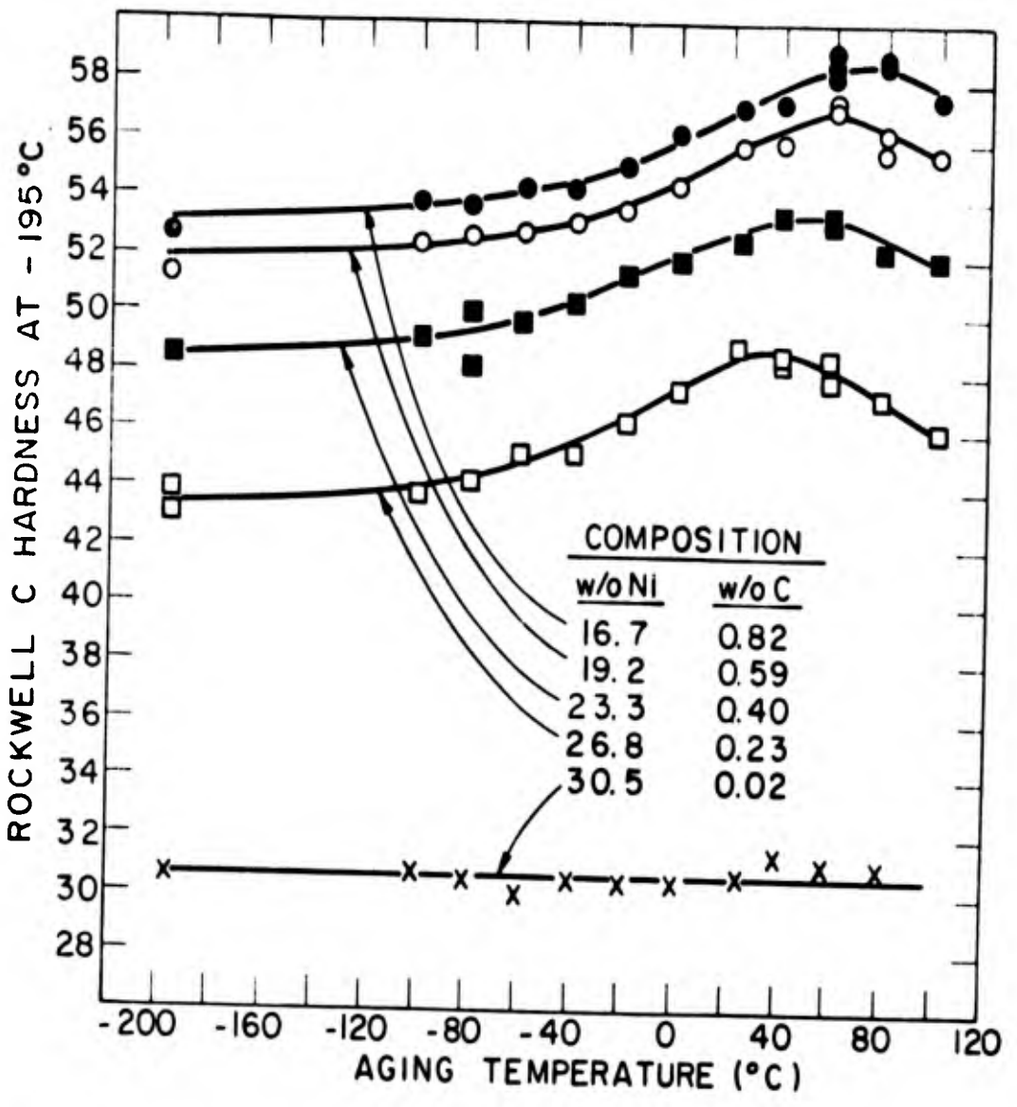

Fig. 8 Rockwell C Hardness of Iron - Nickel - Carbon Martensites as Measured at -195°C after Aging for Three Hours at the Temperatures Shown.

BASIC DISTRIBUTION LIST

Technical and Summary Reports

Organization	No. of Copies
Chief of Naval Research Department of the Navy Washington 25, D.C. Attn: Code 423	(2)
Commanding Officer Office of Naval Research Branch Office 346 Broadway New York 13, New York	(1)
Commanding Officer Office of Naval Research Branch Office 495 Summer Street Boston 10, Mass.	(1)
Commanding Officer Office of Naval Research Branch Office 86 E. Randolph Street Chicago 1, Illinois	(1)
Commanding Officer Office of Naval Research Branch Office 1030 E. Green Street Pasadena 1, California	(1)
Commanding Officer Office of Naval Research Branch Office 1000 Geary Street San Francisco 9, California	(1)
Assistant Naval Attache for Res. Office of Naval Research Branch Office, London Navy 100, Box 39 F.P.O., New York, New York	(5)
Director U.S. Naval Research Laboratory Washington 25, D.C. Attn: Technical Information Officer Code 2000 : Code 2020 : Code 6200 : Code 6300 : Code 6100	(6) (1) (1) (2) (1)

Organization	No. of Copies
Chief, Bureau of Naval Weapons Department of the Navy Washington 25, D.C. Attn: Code RRMA : Code RREN-6	1) 1)
Commanding Officer U.S. Naval Air Material Center Philadelphia, Pennsylvania Attn: Aeronautical Materials Lab.	1)
Superintendent U.S. Naval Weapons Factory Washington 25, D.C. Attn: Code 720	(1)
Commanding Officer U.S. Naval Ordnance Laboratory White Oaks, Maryland	(1)
Commanding Officer U.S. Naval Proving Ground Dahlgren, Virginia Attn: Laboratory Division	1)
Chief, Bureau of Ships Department of the Navy Washington 25, D.C. Attn: Code 330 : Code 337L : Code 343	1) 1) 1)
Commanding Officer U.S. Naval Engineering Experiment Station Annapolis, Maryland Attn: Metals Laboratory	1)
Materials Laboratory New York Naval Shipyard Brooklyn 1, New York Attn: Code 907	1)
Chief, Bureau of Yards and Docks Department of the Navy Washington 25, D.C. Attn: Research and Standards Div.	1)
Commanding Officer David Taylor Model Basin Washington 7, D.S.	.)

BASIC DISTRIBUTION LIST (Continued)

Organization	No. of Copies
Post Graduate School U.S. Naval Academy Monterey, California Attn: Dept. of Metallurgy	(1)
Office of Technical Services Department of Commerce Washington 25, D.C.	(1)
Commanding Officer U.S. Naval Ordnance Test Station Inyokern, California	(1)
Armed Services Technical Information Agency (ASTIA) Documents Service Center Arlington Hall Station Arlington, Va.	(5)
Commanding Officer Watertown Arsenal Watertown, Massachusetts Attn: Ordnance Materials Research Office : Laboratory Division	(1) (1)
Commanding Officer Office of Ordnance Research Box CM, Duke Station Duke University Durham, North Carolina Attn: Metallurgy Division	(1)
Commander Wright Air Development Center Wright-Patterson Air Force Base Dayton, Ohio Attn: Aeronautical Research Lab. (WCRRH) : Aeronautical Research Lab. (WCRRL) : Materials Lab. (WCRTL)	(1) (1) (1)
U.S. Air Force ARDC Office of Scientific Research Washington 25, D.C. Attn: Solid State Division (SRQB)	(1)

Organization	No. of Copies
National Bureau of Standards Washington 25, D.C. Attn: Metallurgy Division : Mineral Products Division	(1) (1)
National Aeronautics Space Administration Lewis Flight Propulsion Laboratory Cleveland, Ohio Attn: Materials and Thermodynamics Division	1)
U.S. Atomic Energy Commission Washington 25, D.C. Attn: Technical Library	1)
U.S. Atomic Energy Commission Washington 25, D.C. Attn: Metals and Materials Branch Division of Research : Eng. Develop. Branch, Division of Reactor Develop.	(1) (1)
Argonne National Laboratory P.O. Box 299 Lemont, Illinois Attn: H. D. Young, Librarian	(1)
Brookhaven National Laboratory Technical Information Division Upton, Long Island, New York Attn: Research Library	1)
Union Carbide Nuclear Co. Oak Ridge National Laboratory P.O. Box P Oak Ridge, Tennessee Attn: Metallurgy Division : Solid State Physics Div. : Laboratory Records Dept.	1) 1) 1)
Los Alamos Scientific Laboratory P.O. Box 1663 Los Alamos, New Mexico Attn: Report Librarian	1)
General Electric Company P.O. Box 100 Richland, Washington Attn: Technical Information Div.	1)

BASIC DISTRIBUTION LIST (Continued)

Organization	No. of Copies
Iowa State College P.O. Box 14A, Station A Ames, Iowa Attn: F. H. Spedding	(1)
U.S. Atomic Energy Commission New York Operations Office 70 Columbus Avenue New York 23, New York Attn: Document Custodian	(1)
Knolls Atomic Power Laboratory P.O. Box 1072 Schenectady, New York Attn: Document Librarian	(1)
Sandia Corporation Sandia Base Albuquerque, New Mexico Attn: Library	(1)
U.S. Atomic Energy Commission Technical Information Service Ext. P.O. Box 62 Oak Ridge, Tennessee Attn: Reference Branch	(1)
University of California Radiation Laboratory Information Division Room 128, Building 50 Berkeley, California Attn: R. K. Wakerling	(1)
Bettis Plant U.S. Atomic Energy Commission Bettis Field P.O. Box 1468 Pittsburgh 30, Pennsylvania Attn: Mrs. Virginia Sternberg, Librarian	(1)
Commanding Officer and Director U.S. Naval Civil Engineering Lab. Port Hueneme, California	(1)
U.S. Bureau of Mines Washington 25, D.C. Attn: Dr. E. T. Hayes	(1)

Organization	No. of Copies
Commanding Officer U.S. Naval Ordnance Underwater Station NewPort, Rhode Island	(1)
Defense Metals Information Center Battelle Memorial Institute 505 King Avenue Columbus, Ohio	(2)
Solid State Devices Branch Evans Signal Laboratory U.S. Army Signal Engineering Labs. c/o Senior Navy Liaison Officer U.S. Navy Electronic Office Fort Monmouth, New Jersey	(1)
U.S. Bureau of Mines P.O. Drawer B Boulder City, Nevada Attn: Electro-Metallurgical Div.	(1)
Commanding General U.S. Army Ordnance Arsenal, Frankford Philadelphia 37, Pennsylvania Attn: Mr. Harold Markus ORDBA-1320, 64-4	(1)

SUPPLEMENTARY DISTRIBUTION LIST

Technical and Summary Reports

Prof. M. Cohen
Department of Metallurgy
Massachusetts Institute of Technology
Cambridge 39, Massachusetts

Prof. B. L. Averbach
Department of Metallurgy
Massachusetts Institute of Technology
Cambridge 39, Massachusetts

Prof. G. M. Pound
Department of Metallurgical Engineering
Carnegie Institute of Technology
Pittsburgh 13, Pennsylvania

Prof. B. E. Warren
Department of Metallurgy
Massachusetts Institute of Technology
Cambridge 39, Massachusetts

Prof. R. F. Hehemann
Department of Metallurgical Engineering
Case Institute of Technology
Cleveland 6, Ohio

Prof. G. C. Kuczynski
Department of Metallurgy
University of Notre Dame
Notre Dame, Indiana

Prof. J. M. Sivertsen
Department of Metallurgy
University of Minnesota
Minneapolis, Minnesota

Prof. P. Duwez
Division of Engineering
California Institute of Technology
Pasadena, California

Prof. V. G. Macres
Department of Metallurgical Engineering
Stanford University
Stanford, California

Prof. L. V. Azaroff
Department of Metallurgical Engineering
Illinois Institute of Technology
Chicago 16, Illinois

Prof. F. Seitz
Department of Physics
University of Illinois
Urbana, Illinois

Prof. T. A. Read
Department of Mining & Met. Engrg.
University of Illinois
Urbana, Illinois

Prof. R. Smoluchowski
Department of Mechanical Engineerin
Princeton University
Princeton, New Jersey

Prof. H. Brooks
Dean of Graduate School of
Applied Science
Harvard University
Cambridge, Massachusetts

Prof. C. E. Birchenall
Department of Chemistry
University of Delaware
Newark, Delaware

Prof. W. E. Wallace
Department of Chemistry
University of Pittsburgh
Pittsburgh 13, Pennsylvania

UNCLASSIFIED